Lawrence Berkeley National Laboratory
Recent Work

Title
First Results from CUORE: A Search for Lepton Number Violation via 0νββ Decay of ^{130}Te.

Permalink
https://escholarship.org/uc/item/6878h66t

Journal
Physical review letters, 120(13)

ISSN
0031-9007

Authors
Alduino, C
Alessandria, F
Alfonso, K
et al.

Publication Date
2018-03-01

DOI
10.1103/physrevlett.120.132501

Peer reviewed

eScholarship.org Powered by the California Digital Library
University of California

First Results from CUORE: A Search for Lepton Number Violation via $0\nu\beta\beta$ Decay of ^{130}Te

C. Alduino,[1] K. Alfonso,[2] E. Andreotti,[3,4,a] C. Arnaboldi,[5] F. T. Avignone III,[1] O. Azzolini,[6] I. Bandac,[1] T. I. Banks,[7,8] G. Bari,[9] M. Barucci,[10,11,b] J.W. Beeman,[12] F. Bellini,[13,14] G. Benato,[7] A. Bersani,[15] D. Biare,[8] M. Biassoni,[4] A. Branca,[16] C. Brofferio,[5,4] A. Bryant,[8,7,c] A. Buccheri,[14] C. Bucci,[17] C. Bulfon,[14] A. Camacho,[6] A. Caminata,[15] L. Canonica,[18,17] X. G. Cao,[19] S. Capelli,[5,4] M. Capodiferro,[14] L. Cappelli,[7,8,17] L. Cardani,[14] P. Carniti,[5,4] M. Carrettoni,[5,4] N. Casali,[14] L. Cassina,[5,4] G. Ceruti,[4] A. Chiarini,[9] D. Chiesa,[5,4] N. Chott,[1] M. Clemenza,[5,4] S. Copello,[20,15] C. Cosmelli,[13,14] O. Cremonesi,[4,d] C. Crescentini,[9] R. J. Creswick,[1] J. S. Cushman,[21] A. D'Addabbo,[17] D. D'Aguanno,[17,22] I. Dafinei,[14] C. J. Davis,[21] F. Del Corso,[9] S. Dell'Oro,[23,17,24] M. M. Deninno,[9] S. Di Domizio,[20,15] M. L. Di Vacri,[17,25] L. Di Paolo,[8,e] A. Drobizhev,[7,8] L. Ejzak,[26,f] R. Faccini,[13,14] D. Q. Fang,[19] M. Faverzani,[5,4] E. Ferri,[4] F. Ferroni,[13,14] E. Fiorini,[4,5] M. A. Franceschi,[27] S. J. Freedman,[8,7,g] B. K. Fujikawa,[8] A. Giachero,[5,4] L. Gironi,[5,4] A. Giuliani,[28] L. Gladstone,[18] J. Goett,[17,h] P. Gorla,[17] C. Gotti,[5,4] C. Guandalini,[9] M. Guerzoni,[9] T. D. Gutierrez,[29] E. E. Haller,[12,30] K. Han,[31] E. V. Hansen,[18,2,i] K. M. Heeger,[21] R. Hennings-Yeomans,[7,8] K. P. Hickerson,[2] H. Z. Huang,[2] M. Iannone,[14] R. Kadel,[32] G. Keppel,[6] L. Kogler,[8,7] Yu. G. Kolomensky,[7,8] A. Leder,[18] C. Ligi,[27] K. E. Lim,[21] Y. G. Ma,[19] C. Maiano,[5,4,j] L. Marini,[20,15] M. Martinez,[13,14,33] C. Martinez Amaya,[1] R. H. Maruyama,[21] Y. Mei,[8] N. Moggi,[34,9] S. Morganti,[14] P. J. Mosteiro,[14] S. S. Nagorny,[17,24] T. Napolitano,[27] M. Nastasi,[5,4] C. Nones,[35] E. B. Norman,[36,37] V. Novati,[28] A. Nucciotti,[5,4] I. Nutini,[17,24] T. O'Donnell,[23] E. Olivieri,[10,11,k] F. Orio,[14] J. L. Ouellet,[18] C. E. Pagliarone,[17,22] M. Pallavicini,[20,15] V. Palmieri,[6] L. Pattavina,[17] M. Pavan,[5,4] M. Pedretti,[36] A. Pelosi,[14] G. Pessina,[4] V. Pettinacci,[14] G. Piperno,[13,14,l] C. Pira,[6] S. Pirro,[17] S. Pozzi,[5,4] E. Previtali,[4] F. Reindl,[14] F. Rimondi,[34,9,g] L. Risegari,[10,11,m] C. Rosenfeld,[1] C. Rusconi,[1,17] M. Sakai,[2] E. Sala,[5,4,n] C. Salvioni,[3,4] S. Sangiorgio,[36] D. Santone,[17,25] D. Schaeffer,[5,4,o] B. Schmidt,[8] J. Schmidt,[2] N. D. Scielzo,[36] V. Singh,[7] M. Sisti,[5,4] A. R. Smith,[8] F. Stivanello,[6] L. Taffarello,[16] M. Tenconi,[28] F. Terranova,[5,4] C. Tomei,[14] G. Ventura,[10,11,p] M. Vignati,[14] S. L. Wagaarachchi,[7,8] B. S. Wang,[36,37] H. W. Wang,[19] B. Welliver,[8] J. Wilson,[1] K. Wilson,[1] L. A. Winslow,[18] T. Wise,[21,26] L. Zanotti,[5,4] G. Q. Zhang,[19] B. X. Zhu,[2,q] S. Zimmermann,[38] and S. Zucchelli[34,9]

(CUORE Collaboration)

[1] *Department of Physics and Astronomy, University of South Carolina, Columbia, SC 29208, USA*
[2] *Department of Physics and Astronomy, University of California, Los Angeles, CA 90095, USA*
[3] *Dipartimento di Fisica e Matematica, Università dell'Insubria, Como I-22100, Italy*
[4] *INFN – Sezione di Milano Bicocca, Milano I-20126, Italy*
[5] *Dipartimento di Fisica, Università di Milano-Bicocca, Milano I-20126, Italy*
[6] *INFN – Laboratori Nazionali di Legnaro, Legnaro (Padova) I-35020, Italy*
[7] *Department of Physics, University of California, Berkeley, CA 94720, USA*
[8] *Nuclear Science Division, Lawrence Berkeley National Laboratory, Berkeley, CA 94720, USA*
[9] *INFN – Sezione di Bologna, Bologna I-40127, Italy*
[10] *Dipartimento di Fisica, Università di Firenze, Firenze I-50125, Italy*
[11] *INFN – Sezione di Firenze, Firenze I-50125, Italy*
[12] *Materials Science Division, Lawrence Berkeley National Laboratory, Berkeley, CA 94720, USA*
[13] *Dipartimento di Fisica, Sapienza Università di Roma, Roma I-00185, Italy*
[14] *INFN – Sezione di Roma, Roma I-00185, Italy*
[15] *INFN – Sezione di Genova, Genova I-16146, Italy*
[16] *INFN – Sezione di Padova, Padova I-35131, Italy*
[17] *INFN – Laboratori Nazionali del Gran Sasso, Assergi (L'Aquila) I-67100, Italy*
[18] *Massachusetts Institute of Technology, Cambridge, MA 02139, USA*
[19] *Shanghai Institute of Applied Physics, Chinese Academy of Sciences, Shanghai 201800, China*
[20] *Dipartimento di Fisica, Università di Genova, Genova I-16146, Italy*
[21] *Wright Laboratory, Department of Physics, Yale University, New Haven, CT 06520, USA*
[22] *Dipartimento di Ingegneria Civile e Meccanica, Università degli Studi di Cassino e del Lazio Meridionale, Cassino I-03043, Italy*
[23] *Center for Neutrino Physics, Virginia Polytechnic Institute and State University, Blacksburg, Virginia 24061, USA*
[24] *INFN – Gran Sasso Science Institute, L'Aquila I-67100, Italy*
[25] *Dipartimento di Scienze Fisiche e Chimiche, Università dell'Aquila, L'Aquila I-67100, Italy*
[26] *Department of Physics, University of Wisconsin, Madison, WI 53706, USA*
[27] *INFN – Laboratori Nazionali di Frascati, Frascati (Roma) I-00044, Italy*
[28] *CSNSM, Univ. Paris-Sud, CNRS/IN2P3, Universit Paris-Saclay, 91405 Orsay, France*
[29] *Physics Department, California Polytechnic State University, San Luis Obispo, CA 93407, USA*

arXiv:1710.07988v1 [nucl-ex] 22 Oct 2017

[30]Department of Materials Science and Engineering,
University of California, Berkeley, CA 94720, USA
[31]INPAC and School of Physics and Astronomy,
Shanghai Jiao Tong University; Shanghai Laboratory for Particle Physics and Cosmology, Shanghai 200240, China
[32]Physics Division, Lawrence Berkeley National Laboratory, Berkeley, CA 94720, USA
[33]Laboratorio de Fisica Nuclear y Astroparticulas,
Universidad de Zaragoza, Zaragoza 50009, Spain
[34]Dipartimento di Fisica e Astronomia, Alma Mater Studiorum – Università di Bologna, Bologna I-40127, Italy
[35]Service de Physique des Particules, CEA / Saclay, 91191 Gif-sur-Yvette, France
[36]Lawrence Livermore National Laboratory, Livermore, CA 94550, USA
[37]Department of Nuclear Engineering, University of California, Berkeley, CA 94720, USA
[38]Engineering Division, Lawrence Berkeley National Laboratory, Berkeley, CA 94720, USA
(Dated: October 24, 2017)

The CUORE experiment, a ton-scale cryogenic bolometer array, recently began operation at the Laboratori Nazionali del Gran Sasso in Italy. The array represents a significant advancement in this technology, and in this work we apply it for the first time to a high-sensitivity search for a lepton-number–violating process: ^{130}Te neutrinoless double-beta decay. Examining a total TeO_2 exposure of 86.3 kg·yr, characterized by an effective energy resolution of (7.7 ± 0.5) keV FWHM and a background in the region of interest of (0.014 ± 0.002) counts/(keV·kg·yr), we find no evidence for neutrinoless double-beta decay. The median statistical sensitivity of this search is 7.0×10^{24} yr. Including systematic uncertainties, we place a lower limit on the decay half-life of $T^{0\nu}_{1/2}(^{130}\mathrm{Te}) > 1.3 \times 10^{25}$ yr (90% C.L.). Combining this result with those of two earlier experiments, Cuoricino and CUORE-0, we find $T^{0\nu}_{1/2}(^{130}\mathrm{Te}) > 1.5 \times 10^{25}$ yr (90% C.L.), which is the most stringent limit to date on this decay. Interpreting this result as a limit on the effective Majorana neutrino mass, we find $m_{\beta\beta} < (140 - 400)$ meV, where the range reflects the nuclear matrix element estimates employed.

The existence of nonzero neutrino masses has been well established by precision measurements of neutrino flavor oscillation [1]. This discovery has given renewed impetus to long-standing questions as to the Dirac or Majorana nature of the neutrino [2], the role of Majorana neutrinos in cosmological evolution [3], and the absolute neutrino mass scale. Neutrinoless double-beta ($0\nu\beta\beta$) decay is a lepton-number–violating process that can occur only if neutrinos are Majorana fermions [4–7]. The discovery of this decay would unambiguously demonstrate that lepton number is not a symmetry of nature and that neutrinos are Majorana particles; additionally, a measurement of the decay rate may constrain the absolute neutrino mass scale. These fundamental implications drive considerable effort worldwide to search for this decay [8].

If it occurs, $0\nu\beta\beta$ decay would have a robust experimental signature: a peak in the summed energy spectrum of the final state electrons at the Q-value of the decay ($Q_{\beta\beta}$). To maximize its sensitivity to this signature, an experiment must have a low background rate near $Q_{\beta\beta}$, good energy resolution, and a large source mass. The Cryogenic Underground Observatory for Rare Events (CUORE) [9] is a new detector that applies the powerful macro-bolometer technique [10, 11] at an unprecedented scale to the search for the $0\nu\beta\beta$ decay of tellurium isotopes. In this work, we focus on the $0\nu\beta\beta$ decay of ^{130}Te to the ground state of ^{130}Xe. Our sensitivity benefits from the high natural abundance of ^{130}Te, (34.167 ± 0.002)% [12], and large $Q_{\beta\beta}$ of (2527.515 ± 0.013) keV [13–15].

CUORE is composed of 988 $5 \times 5 \times 5$ cm^3 TeO_2 crystals [16], which we can cool to temperatures as low as 7 mK. When a crystal absorbs energy, the resulting temperature increase provides a measure of the energy deposited. Each crystal is instrumented with a neutron-transmutation-doped germanium thermistor [17], to record thermal pulses, and a silicon heater [18, 19], across which reference pulses are applied for thermal gain stabilization. The operating temperature is a compromise between minimizing the heat capacity of the crystals, thus maximizing the thermal gain, and optimizing the signal bandwidth.

The 988 TeO_2 crystals are arranged into 19 copper-framed towers, with each tower consisting of 13 floors of 4 crystals each. The crystals in each tower are held in the frame by polytetrafluoroethylene supports. The towers are arranged in a close-packed array and thermally connected to the mixing chamber of a ^{3}He/^{4}He dilution refrigerator[20]. Precooling to maintain the dilution cycle is realized by five two-stage ($\sim$40 K and $\sim$4 K) pulse tube cryocoolers [21] and a Joule-Thomson expansion valve. The dimensions, experimental volume ($\sim$1 m^3), mass ($\sim$17 t), and cooling power (3 μW at 10 mK) make this the largest and most powerful cryogen-free dilution cryostat in operation [22]. To minimize transmission of vibrations from the cryostat to the bolometers, the detector towers are independently supported by a Y-shaped beam that is vibrationally isolated from the cryostat support structure [23]. The cryostat and detector supports and front-end electronics are located together in a Faraday Room [24].

To suppress external γ-ray backgrounds, two lead

shields are integrated into the cryogenic volume: a 30-cm thick shield at ∼50 mK above the detectors and a 6-cm thick shield at ∼4 K around and below the detectors. The lateral and lower shields are made from ancient Roman lead with extremely low levels of radioactivity [25]. In addition, an external lead shield (70 t, 25 cm thick) surrounded by borated polyethylene and boric acid 6 t, 20 cm thick) is raised around the outermost cryostat vessel during data collection.

A prototype detector equivalent to a single CUORE tower, CUORE-0, operated as a standalone experiment at the Laboratori Nazionali del Gran Sasso from 2013 to 2015 and served to validate the material selection program and low-background assembly techniques developed for CUORE [16, 26–29]. Prior to the current work, the strongest probe of $\beta\beta$ decay of ^{130}Te came from CUORE-0 [30–32].

The data we present here are from two month-long datasets collected from May to June and August to September of 2017. Between the two datasets, we improved the detector operating conditions; in particular, we implemented an active noise cancellation system on the pulse tube cryocoolers [33] and improved the electrical grounding of the experiment. To select the optimal operating temperature, we performed a temperature scan to study the energy resolution achieved by a representative subset of detectors. An operating temperature of approximately 15 mK was selected for both datasets.

Each dataset is bookended by periods devoted to energy calibration with ^{232}Th γ-ray sources; the closing calibration is performed to verify the stability of the detector response over the dataset. During calibration, to achieve efficient and approximately uniform γ-ray illumination of the detectors, we temporarily lower 12 Kevlar strings populated with low-intensity ^{232}Th sources from room temperature into the cryogenic volume amongst and around the towers [34]. We use the data collected between calibrations, which we refer to as *physics data*, for our $0\nu\beta\beta$ decay search.

During data collection, the voltage across each thermistor is amplified and filtered [35–38] and continuously digitized with a sampling rate of 1 kHz [39–41]. A total of 984 of 988 channels are functioning. Thermal event pulses are identified by a software derivative trigger with channel-dependent thresholds ranging from 20 to a few hundred keV; we anticipate reducing these thresholds for future low-energy studies [42, 43]. The rise and fall times of thermal pulses are on the order of 100 ms and 400 ms, respectively. Once an event pulse is triggered, we analyze a 10-s window consisting of 3 s before and 7 s after each trigger. The pre-trigger voltage provides a proxy for the bolometer temperature before the event, while the pulse amplitude establishes the energy of the event. The average event rate per detector is ∼50 mHz in calibration data and ∼6 mHz in physics data. In addition to triggered pulses, every few minutes the silicon heater on each bolometer is injected with a stable voltage pulse [44] to generate tagged reference events with fixed thermal energy. To monitor and characterize noise we also analyze waveforms that do not contain discernible thermal pulses.

To improve the signal-to-noise ratio, we apply an optimal filter to each pulse [45], exploiting the distinct frequency characteristics of particle-induced and noise waveforms. The pulse amplitude is determined from the maximum value attained by the filtered waveform. To monitor and correct for possible drifts in the energy-to-amplitude response of the detection chain (e.g., due to small drifts in operating temperature), which could otherwise spoil the energy resolution of our detectors, we apply thermal gain stabilization (TGS) to each event amplitude. We apply one of two methods: the first uses monoenergetic heater pulses with ∼1 ppm absolute stability [44] (heater-TGS) and the second uses pulses induced by γ rays from the 2615-keV ^{208}Tl calibration line (calibration-TGS). Both methods were developed and used in CUORE-0 [31]. Heater-TGS is our default algorithm, while we use calibration-TGS for the ∼3% of bolometers without functioning heaters and for channels in which calibration-TGS yields a statistically significant improvement in sensitivity compared to heater-TGS. In total, 96.6% of our exposure utilizes heater-TGS while the remainder uses calibration-TGS.

To calibrate the detectors, we use six γ lines from the ^{232}Th calibration sources ranging from 239 keV to 2615 keV. We estimate the mean stabilized amplitude of each line and create a calibration function for each bolometer in each dataset (each *bolometer–dataset*), which maps stabilized pulse amplitudes to physical energies. We find that the calibration functions of each bolometer–dataset are well described by a second-order polynomial with zero constant term throughout the calibrated energy range. After calibrating, we blind the data for the subsequent analysis by introducing an artificial peak at $Q_{\beta\beta}$ [31]. The calibration and unblinded physics spectra are shown in Figure 1.

To select $0\nu\beta\beta$ decay candidates in the physics data, we apply a series of selection criteria. We begin by discarding noisy periods of data caused by conditions in the laboratory. This reduces the total exposure by 1%. Following this, we apply basic pulse quality selection to each event, requiring a single pulse-like feature in the event window and a stable thermistor voltage prior to the event trigger. We then require the shape of each waveform to be consistent with that of a true signal-like event. We build a signal-like event sample in physics data from events that reconstruct within 10 keV of the γ lines from ^{40}K at 1461 keV and ^{60}Co at 1173 keV and 1332 keV. We characterize event waveforms with six pulse-shape parameters and represent each event with a point in this 6-dimensional space. We calculate the Mahalanobis distance D_M [46] for each event from the mean position of the signal sample. We choose the upper limit on D_M that

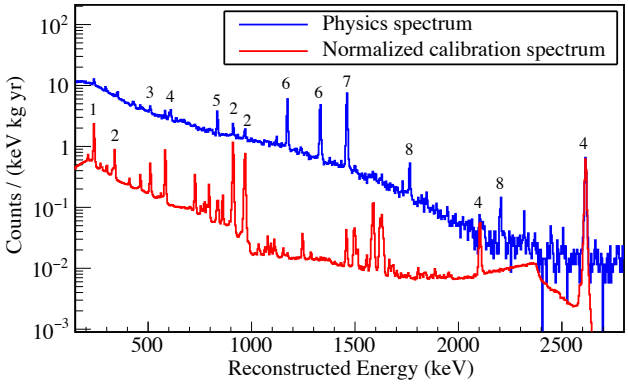

FIG. 1. Reconstructed energy spectra of physics (blue) and calibration (red) data. The calibration spectrum is normalized to the physics data at the 2615-keV line. The sources of the labeled peaks are identified as: (1) ^{212}Pb, (2) ^{228}Ac, (3) e^+e annihilation, (4) ^{208}Tl, (5) ^{54}Mn, (6) ^{60}Co, (7) ^{40}K, (8) ^{214}Bi.

TABLE I. Event selection efficiencies and performance parameters for the two datasets analyzed in this work. The effective resolution and background parameters are given at $Q_{\beta\beta}$. The uncertainty on exposure is negligible.

	Dataset 1	Dataset 2
Selection Efficiency (%)		
Base	95.63 ± 0.01	96.69 ± 0.01
Pulse shape (D_M)	91.1 ± 3.6	98.2 ± 3.0
Anti-coincidence (accidental)	99.4 ± 0.5	100.0 ± 0.4
Anti-coincidence ($\beta\beta$ containment)	88.35 ± 0.09	
Total (excl. $\beta\beta$ containment)	85.7 ± 3.4	94.0 ± 2.9
Performance Parameters		
Channels used	876	935
TeO_2 exposure (kg·yr)	37.6	48.7
Effective resolution (keV)	8.3 ± 0.4	7.4 ± 0.7
Background (10^{-2} c/(keV·kg·yr))	1.49 ± 0.18	1.35 ± 0.19

maximizes the discovery sensitivity [47]; throughout this optimization, data from the region of interest for $0\nu\beta\beta$ decay are not used, and the efficiency of the D_M selection condition used in the sensitivity calculation is estimated from ^{40}K events near 1461 keV. Once the optimal upper limit on D_M is chosen, we evaluate the efficiency of the pulse shape selection using events belonging to the ^{208}Tl 2615-keV line.

To reduce backgrounds from decays depositing energy in multiple crystals (e.g., α particles on crystal surfaces or multiple Compton scatters of γ rays), we reject events that occur within 10 ms of an event in a different bolometer in the array, which we refer to as anti-coincidence selection. The width of the coincidence window is chosen after correcting for differences in detector rise times and trigger configurations that can affect the timestamp assigned to an event. The inter-bolometer timestamp differences are determined using physically coincident multi-detector events, such as pair-production events, occurring in calibration data. The energy threshold for coincident events in this analysis is set to 150 keV; we expect to lower this in the future as we improve the operating conditions of the experiment. The anti-coincidence selection efficiency has two components: the probability for a $0\nu\beta\beta$ decay to be fully contained in a single crystal and the probability for it to not be accidentally coincident with another event and thus removed from the data. We estimate the former from simulation [48, 49] and the latter we determine using the 1461-keV γ ray from ^{40}K electron capture, which is a single-event decay that is not expected to produce physical coincidences.

We evaluate the trigger efficiency as the fraction of tagged heater pulses that produce an event trigger. We also exploit heater events to measure the basic pulse quality selection efficiency mentioned above and the energy reconstruction efficiency (i.e., the probability that a monoenergetic pulse reconstructs correctly). The combined trigger, basic pulse quality, and reconstruction efficiency, denoted by *base efficiency*, is averaged over all channels with functioning heaters and applied to all channels. In cases where a step in the event reconstruction procedure fails for a given channel, we remove that channel from the subsequent analysis. The number of channels studied and the $0\nu\beta\beta$ decay candidate selection efficiencies are summarized in Table I.

We establish the detector response to a monoenergetic event near $Q_{\beta\beta}$ using the high-statistics ^{208}Tl 2615-keV γ line from calibration data. The CUORE detectors exhibit a slightly non-Gaussian line shape, as was observed in CUORE-0 [31] and Cuoricino [50, 51]. The origin of this structure is under investigation; however, we model it empirically with a primary Gaussian component centered at 2615 keV and two additional Gaussian components, one on the right and one on the left of the main peak. We find this model provides a better description of the data compared to other models considered, for example a single- or double-Gaussian photopeak. The choice of line shape is treated as a systematic uncertainty, which we discuss below. All three Gaussian components are parametrized with the same bolometer–dataset dependent width. We estimate the line shape parameters for each bolometer–dataset in each tower with a simultaneous, unbinned extended maximum likelihood (UEML) fit performed on that tower in the energy range 2530–2720 keV[52]. A comparison of the results of these fits with the calibration data is shown in Figure 2.

To allow for possible systematic differences in the detector energy resolution due to the higher event rate during calibration, we apply a dataset-dependent scaling fac-

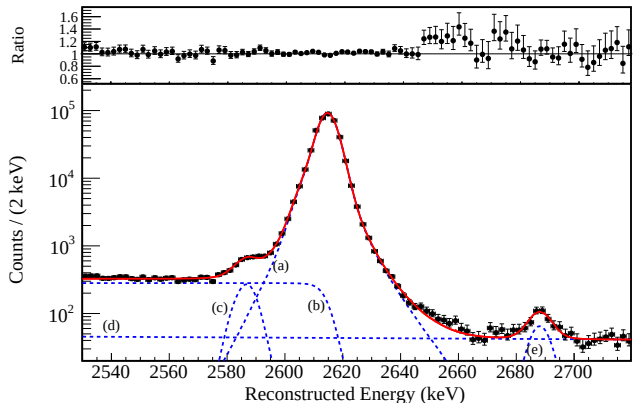

FIG. 2. Bottom: Sum of the results of the 19 tower-dependent UEML fits we use to estimate the line shape parameters of each bolometer–dataset in calibration data. The solid red line is the sum of the best-fit line shape model of each bolometer–dataset; the components of this summed best-fit model are shown by the blue dashed lines. We identify (a) the multi-Gaussian photopeak that describes the detector response function, (b) a multiscatter Compton contribution, (c) multiple peaks due to 27–31 keV Te X-ray escape following an incident 2615-keV γ ray, (d) a linear continuum background due to coincident events, and (e) a line due to coincident absorption of 2615-keV and 583-keV γ rays from the ^{232}Th decay chain followed by escape of a 511-keV annihilation γ from pair production. Top: Ratio between calibration data and line shape model.

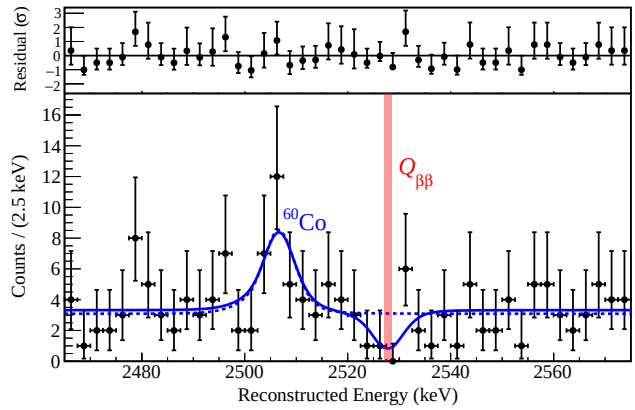

FIG. 3. Bottom: Best-fit model from the UEML fit (solid blue line) overlaid on the spectrum of $0\nu\beta\beta$ decay candidates observed in CUORE. The peak near 2506 keV is attributed to ^{60}Co [31]. The normalized residuals of this model and the binned data are shown in the top panel. The dashed (blue) curve shows the best-fit for a model with no $0\nu\beta\beta$ decay component. The vertical band is centered at $Q_{\beta\beta}$; the width of the band reflects the systematic uncertainty on the reconstructed energy.

tor to the width parameter for each bolometer–dataset. These scaling parameters and their energy dependence, which we model as a quadratic function, are determined from a simultaneous UEML fit to the 2615-keV line and other prominent lines in the physics spectrum. The best-fit scaling parameters at 2615 keV are 0.95 ± 0.07 and 1.01 ± 0.06 for the first and second dataset, respectively. The exposure-weighted harmonic mean energy resolution (denoted by *effective resolution*) in physics data, extrapolated to $Q_{\beta\beta}$, is given for each dataset in Table I; to quote a single characteristic energy resolution for our entire exposure, we combine these, finding a resolution of (7.7 ± 0.5) keV FWHM.

Before unblinding the physics data, we fix the model and fitting strategy to search for the $0\nu\beta\beta$ decay of ^{130}Te. The region of interest (ROI) is 2465 keV to 2575 keV, approximately centered on $Q_{\beta\beta}$. The model for each bolometer–dataset is composed of a posited $0\nu\beta\beta$ decay peak, a peak for ^{60}Co coincident γ rays (1173 and 1332 keV), and a flat background. Each peak is modeled using the calibration line shape discussed above, with the line width scaled by the resolution scaling parameter extrapolated to the peak energy. All detectors are constrained to have the same $0\nu\beta\beta$ decay rate $\Gamma_{0\nu}$, which we allow to vary freely in the fit; the position of the $0\nu\beta\beta$ decay peak is fixed to the reconstructed energy of $Q_{\beta\beta}$ for each bolometer-dataset. Comparing the mean reconstructed energy of γ peaks in the physics data spectrum to their known energies, we find the energy reconstruction bias is less than ± 0.5 keV throughout the calibrated energy range; we propagate this maximum bias as a systematic uncertainty. The ^{60}Co peak mean, ^{60}Co rate, and flat background rate are free parameters in the fit. The background rate is dataset-dependent and is not scaled by the event selection efficiency in the fit.

Figure 3 shows the 155 candidate events in the ROI that pass all selection criteria together with the result of the UEML fit described above. The total TeO_2 exposure is 86.3 kg·yr, corresponding to a ^{130}Te exposure of 24.0 kg·yr. The best-fit $\Gamma_{0\nu}$ is $(-1.0\ ^{+0.4}_{-0.3}\ \text{(stat.)} \pm 0.1\ \text{(syst.)}) \times 10^{-25}$ yr^{-1}. When the $0\nu\beta\beta$ decay component is removed from the model, the best-fit background index in the ROI averaged over both datasets is (0.014 ± 0.002) counts/(keV·kg·yr).

To evaluate the goodness of fit, we prepare a large set of pseudo-experiments, each with a number of events determined by a Poisson distribution with a mean of 155 and energy distributed according to the best-fit zero-signal model. We repeat our $0\nu\beta\beta$ decay search fit on each of these pseudo-experiments and find that 68% yield a negative log likelihood (NLL) larger than that obtained with our data.

We conclude there is no evidence for $0\nu\beta\beta$ decay and set a 90% C.L. upper limit on $\Gamma_{0\nu}$ by integrating the profile likelihood for $\Gamma_{0\nu} \geq 0$. The result is $\Gamma_{0\nu} < 0.50 \times 10^{-25}$ yr^{-1} (stat. only), which corresponds to a half-life of $T^{0\nu}_{1/2} > 1.4 \times 10^{25}$ yr. The median 90%

TABLE II. Systematic uncertainties on $\Gamma_{0\nu}$ for zero signal (additive) and as a percentage of nonzero signal (scaling).

	Additive (10^{-25} yr^{-1})	Scaling (%)
Line shape	0.02	2.4
Energy resolution	–	1.5
Fit bias	–	0.3
Energy scale	–	0.2
Background shape	0.05	0.8
Selection efficiency	2.4%	

C.L. lower limit sensitivity for $T^{0\nu}_{1/2}$ is 7.0×10^{24} yr, and there is a 2% probability of obtaining a more stringent limit.

We estimate the systematic uncertainties following the same procedure used for CUORE-0 [31]. We perform a large number of pseudo-experiments with zero and nonzero signals assuming different detector line shape models and background shapes (flat and first-order polynomial), varying the energy resolution scaling parameters within their uncertainty, and shifting the position of $Q_{\beta\beta}$ by ± 0.5 keV to account for the energy reconstruction uncertainty. The results are summarized in Table II. We find the fit bias on $\Gamma_{0\nu}$ to be negligible. Including these systematic uncertainties, the 90% C.L. limits are $\Gamma_{0\nu} < 0.52 \times 10^{-25}$ yr^{-1} and $T^{0\nu}_{1/2} > 1.3 \times 10^{25}$ yr. We perform the analysis described above with the RooFit toolkit [53] employing the Minuit minimization routines [54]. An independent Bayesian analysis using the BAT toolkit [55], marginalizing over the nuisance parameters and employing a flat prior for $\Gamma_{0\nu} \geq 0$, produces results in agreement with those above. A frequentist analysis [56] yields $T^{0\nu}_{1/2} > 2.1 \times 10^{25}$ yr at 90% C.L. with a median 90% C.L. lower limit sensitivity for $T^{0\nu}_{1/2}$ of 7.6×10^{24} yr.

We combine the profile NLL curve from our primary analysis described above with those from 9.8 kg·yr of ^{130}Te exposure from CUORE-0 [30] and 19.8 kg·yr from Cuoricino [57] (see Figure 4). The combined 90% C.L. limits are $\Gamma_{0\nu} < 0.47 \times 10^{-25}$ yr^{-1} and $T^{0\nu}_{1/2} > 1.5 \times 10^{25}$ yr. The frequentist technique yields $\Gamma_{0\nu} < 0.31 \times 10^{-25}$ yr^{-1} and $T^{0\nu}_{1/2} > 2.2 \times 10^{25}$ yr.

We interpret the combined half-life limit, $T^{0\nu}_{1/2} > 1.5 \times 10^{25}$ yr, as a limit on the effective Majorana neutrino mass ($m_{\beta\beta}$) in the framework of models of $0\nu\beta\beta$ decay mediated by light Majorana neutrino exchange. We use phase-space factors from [58] and nuclear matrix elements from recent calculations using a broad range of models [59–63], and we assume the axial coupling constant $g_A \simeq 1.27$; this yields $m_{\beta\beta} < (140 - 400)$ meV at 90% C.L., depending on the nuclear matrix element estimates employed.

In summary, we find no evidence for $0\nu\beta\beta$ decay of ^{130}Te and place the most stringent limit to date on the half-life for this decay. The observed background index, (0.014 ± 0.002) counts/(keV·kg·yr), is in line with our expectations based on the background model developed in [49]. The characteristic energy resolution of the array at $Q_{\beta\beta}$ is (7.7 ± 0.5) keV, which we foresee improving to ∼5 keV by further optimizing our experimental operating conditions and through analysis improvements currently in development. A study of the future sensitivities for a number of background and energy resolution scenarios is presented in [64]. CUORE is the first ton-scale cryogenic detector array in operation, more than an order of magnitude larger than its predecessors. The successful commissioning and operation of this large-mass, low-background cryogenic bolometer array represents a major advancement in the application of this technique to $0\nu\beta\beta$ decay searches and demonstrates the feasibility of future large-mass bolometer arrays for rare-event searches.

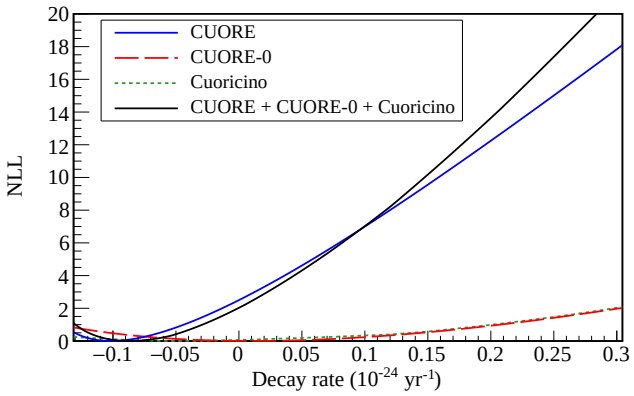

FIG. 4. Profile negative-log-likelihood curves for CUORE, CUORE-0, Cuoricino, and their combination.

The CUORE Collaboration thanks the directors and staff of the Laboratori Nazionali del Gran Sasso and our technical staff for their valuable contribution to building and operating the detector. We thank Danielle Speller for contributions to detector calibration, data analysis, and discussion of the manuscript. We thank Giorgio Frossati for his crucial support in the commissioning of the dilution unit. This work was supported by the Istituto Nazionale di Fisica Nucleare (INFN); the National Science Foundation under Grant Nos. NSF-PHY-0605119, NSF-PHY-0500337, NSF-PHY-0855314, NSF-PHY-0902171, NSF-PHY-0969852, NSF-PHY-1307204, and NSF-PHY-1404205; the Alfred P. Sloan Foundation; and Yale University. This material is also based upon work supported by the US Department of Energy (DOE) Office of Science under Contract Nos. DE-AC02-05CH11231 and DE-AC52-07NA27344; and by the DOE Office of Science, Office of Nuclear Physics under Contract Nos. DE-FG02-08ER41551, DE-FG03-00ER41138, DE-SC0011091, and DE-SC0012654. This research used

resources of the National Energy Research Scientific Computing Center (NERSC).

[a] Present address: University College Leuven-Limburg, 3590 Diepenbeek, Belgium
[b] Present address: Istituto Nazionale di Ottica, Consiglio Nazionale delle Ricerche (INO-CNR), Firenze I-50125, Italy
[c] Applied Physics Laboratory, The Johns Hopkins University, Baltimore, MD 20723, USA
[d] Corresponding author: cuore-spokesperson@lngs.infn.it
[e] Present address: INFN – Laboratori Nazionali del Gran Sasso, Assergi (L'Aquila) I-67100, Italy
[f] Present address: Research Square, Durham, NC 27701, USA
[g] Deceased
[h] Present address: Physics Division, P-23, Los Alamos National Laboratory, Los Alamos, NM 87544, USA
[i] Present address: Department of Physics, Drexel University, Philadelphia, PA 19104, USA
[j] Present address: European Spallation Source (ESS), 225 92 Lund, Sweden
[k] Present address: CSNSM, Univ. Paris-Sud, CNRS/IN2P3, Universit Paris-Saclay, 91405 Orsay, France
[l] Present address: INFN – Laboratori Nazionali di Frascati, Frascati (Roma) I-00044, Italy
[m] Present address: Laboratoire Commun de Métrologie, LNE-CNAM, 93210 La Plaine Saint-Denis, France
[n] Present address: Max-Planck-Institut für Physik, 80805 München, Germany
[o] Present address: ABB Corporate Research Center, 722 26 Västerås, Sweden
[p] Present address: CryoVac GmbH & Co KG, 53842 Troisdorf, Germany
[q] Present address: Los Alamos National Laboratory, Los Alamos, New Mexico 87545, USA

[1] C. Patrignani *et al.* (Particle Data Group), Chin. Phys. C **40**, 100001 (2016).
[2] E. Majorana, Nuovo Cimento **14**, 171 (1937).
[3] M. Fukugita and T. Yanagida, Phys. Lett. B **174**, 45 (1986).
[4] G. Racah, Nuovo Cimento **14**, 322 (1937).
[5] W. H. Furry, Phys. Rev. **56**, 1184 (1939).
[6] B. Pontecorvo, Sov. Phys. JETP **26**, 984 (1968).
[7] J. Schechter and J. Valle, Phys. Rev. D **25**, 2951 (1982).
[8] S. Dell'Oro, S. Marcocci, M. Viel, and F. Vissani, Adv. High Energy Phys. **2016**, 2162659 (2016).
[9] D. R. Artusa *et al.*, Adv. High Energy Phys. **2015**, 879871 (2015).
[10] E. Fiorini and T. Niinikoski, Nucl. Instrum. Meth. **224**, 83 (1984).
[11] C. Enss and D. McCammon, J. Low Temp. Phys. **151**, 5 (2008).
[12] M. A. Fehr, M. Rehkämper, and A. N. Halliday, Int. J. Mass Spectrom. **232**, 83 (2004).
[13] M. Redshaw, B. J. Mount, E. G. Myers, and F. T. Avignone, III, Phys. Rev. Lett. **102**, 212502 (2009).
[14] N. D. Scielzo *et al.*, Phys. Rev. C **80**, 025501 (2009).
[15] S. Rahaman *et al.*, Phys. Lett. B **703**, 412 (2011).
[16] C. Arnaboldi *et al.*, J. Cryst. Growth **312**, 2999 (2010).
[17] E. E. Haller, N. P. Palaio, M. Rodder, W. L. Hansen, and E. Kreysa, in *Neutron Transmutation Doping of Semiconductor Materials* (Springer US, Boston, MA, 1984) pp. 21–36.
[18] A. Alessandrello *et al.*, Nucl. Instrum. Meth. A **412**, 454 (1998).
[19] E. Andreotti *et al.*, Nucl. Instrum. Meth. A **664**, 161 (2012).
[20] Leiden Cryogenics DRS-CF3000 continuous-cycle.
[21] Cryomech PT415-RM.
[22] F. Alessandria *et al.*, "The CUORE cryostat: A 10 mK infrastructure for large bolometric arrays," (In preparation).
[23] A. Bersani *et al.*, "The detector suspension system of the CUORE experiment," (In preparation).
[24] C. Bucci *et al.*, "The Faraday room of the CUORE Experiment," (2017), arXiv:1710.05614.
[25] A. Alessandrello *et al.*, Nucl. Instrum. Meth. **142**, 163 (1998).
[26] F. Alessandria *et al.*, Astropart. Phys. **45**, 13 (2013).
[27] E. Buccheri, M. Capodiferro, S. Morganti, F. Orio, A. Pelosi, and V. Pettinacci, Nucl. Instrum. Meth. A **768**, 130 (2014).
[28] C. Alduino *et al.* (CUORE Collaboration), J. Instrum. **11**, P07009 (2016).
[29] E. Andreotti *et al.*, JINST **4**, P09003 (2009).
[30] K. Alfonso *et al.* (CUORE Collaboration), Phys. Rev. Lett. **115**, 102502 (2015).
[31] C. Alduino *et al.* (CUORE Collaboration), Phys. Rev. C **93**, 045503 (2016).
[32] C. Alduino *et al.* (CUORE Collaboration), Eur. Phys. J. C **77**, 13 (2017).
[33] A. D'Addabbo, C. Bucci, L. Canonica, S. Di Domizio, P. Gorla, L. Marini, and B. Welliver, "An active noise cancellation technique for the CUORE Pulse Tube Cryocoolers," (In preparation).
[34] J. S. Cushman *et al.*, Nucl. Instrum. Meth. A **844**, 32 (2017).
[35] C. Arnaboldi, P. Carniti, L. Cassina, C. Gotti, X. Liu, and G. Pessina, "The front end electronics system for the CUORE experiment," (In preparation).
[36] P. Carniti, L. Cassina, C. Gotti, M. Maino, and G. Pessina, Rev. Sci. Instrum. **87**, 054706 (2016).
[37] C. Arnaboldi *et al.*, Rev. Sci. Instrum. **86**, 124703 (2015).
[38] C. Arnaboldi, M. Cariello, S. Di Domizio, A. Giachero, and G. Pessina, Nucl. Instrum. Meth. A **617**, 327 (2010).
[39] A. Giachero, *Characterization of cryogenic bolometers and data acquisition system for the CUORE experiment*, Ph.D. thesis, Università degli studi di Genova (2008).
[40] S. Di Domizio, *Search for double beta decay to excited states with CUORICINO and data acquisition system for CUORE*, Ph.D. thesis, Università degli studi di Genova (2009).
[41] S. Copello, *Dark Matter Induced Annual Modulation Analysis in CUORE-0*, Ph.D. thesis, Università degli studi di Genova (2017).
[42] S. Di Domizio, F. Orio, and M. Vignati, J. Instrum. **6**, P02007 (2011).
[43] C. Alduino *et al.* (CUORE Collaboration), "Low Energy Analysis Techniques for CUORE," (2017), arXiv:1708.07809.
[44] P. Carniti, L. Cassina, A. Giachero, C. Gotti, and G. Pessina, "A High Precision Pulse Generation and Sta-

bilization System for Bolometric Experiments," (2017), arXiv:1710.05565.
[45] E. Gatti and P. F. Manfredi, Nuovo Cimento **9**, 1 (1986).
[46] P. C. Mahalanobis, Proc. Natl. Inst. Sci. India , 49 (1936).
[47] G. Cowan, K. Cranmer, E. Gross, and O. Vitells, Eur. Phys. J. C **71**, 1554 (2011).
[48] S. Agostinelli *et al.*, Nucl. Instr. Meth. A , 250 (2003).
[49] C. Alduino *et al.* (CUORE Collaboration), Eur. Phys. J. C **77**, 543 (2017).
[50] A. D. Bryant, *A Search for Neutrinoless Double Beta Decay of* ^{130}*Te*, Ph.D. thesis, University of California, Berkeley (2010).
[51] M. Carrettoni, *Data analysis for Neutrinoless Double Beta Decay*, Ph.D. thesis, Università degli Studi di Milano-Bicocca (2011).
[52] A simultaneous fit over the full array was not performed in this analysis for computational convenience.
[53] W. Verkerke and D. P. Kirkby, eConf **C0303241**, MOLT007 (2003), arXiv:physics/0306116.
[54] F. James and M. Roos, Comput. Phys. Commun. **10**, 343 (1975).
[55] A. Caldwell, D. Kollar, and K. Kroninger, Comput. Phys. Commun. **180**, 2197 (2009).
[56] W. A. Rolke, A. M. Lopez, and J. Conrad, Nucl. Instrum. Meth. A **551**, 493 (2005).
[57] E. Andreotti *et al.*, Astropart. Phys. **34**, 822 (2011).
[58] J. Kotila and F. Iachello, Phys. Rev. C **85**, 034316 (2012).
[59] J. Barea, J. Kotila, and F. Iachello, Phys. Rev. C **91**, 034304 (2015).
[60] F. Šimkovic, V. Rodin, A. Faessler, and P. Vogel, Phys. Rev. C **87**, 045501 (2013).
[61] J. Hyvärinen and J. Suhonen, Phys. Rev. C **91**, 024613 (2015).
[62] J. Menendez, A. Poves, E. Caurier, and F. Nowacki, Nucl. Phys. A **818**, 139 (2009).
[63] T. R. Rodriguez and G. Martinez-Pinedo, Phys. Rev. Lett. **105**, 252503 (2010).
[64] C. Alduino *et al.* (CUORE Collaboration), Eur. Phys. J. C **77**, 532 (2017).